Phylogenomics Identifies a New Major Subgroup of Apicomplexans, Marosporida *class nov.*, with Extreme Apicoplast Genome Reduction

Varsha Mathur[1,*], Waldan K. Kwong[1], Filip Husnik [ID][2], Nicholas A.T. Irwin [ID][1], Árni Kristmundsson[3], Camino Gestal[4], Mark Freeman[5], and Patrick J. Keeling[1]

[1]Department of Botany, University of British Columbia, Vancouver, British Columbia, Canada

[2]Okinawa Institute of Science and Technology, Okinawa, Japan

[3]Fish Disease Laboratory, Institute for Experimental Pathology, University of Iceland, Reykjavík, Iceland

[4]Institute of Marine Research (IIM-CSIC), Vigo, Spain

[5]Ross University School of Veterinary Medicine, Basseterre, Saint Kitts and Nevis, West Indies

*Corresponding author: E-mail: varsha.mathur@botany.ubc.ca.

Abstract

The phylum Apicomplexa consists largely of obligate animal parasites that include the causative agents of human diseases such as malaria. Apicomplexans have also emerged as models to study the evolution of nonphotosynthetic plastids, as they contain a relict chloroplast known as the apicoplast. The apicoplast offers important clues into how apicomplexan parasites evolved from free-living ancestors and can provide insights into reductive organelle evolution. Here, we sequenced the transcriptomes and apicoplast genomes of three deep-branching apicomplexans, *Margolisiella islandica*, *Aggregata octopiana*, and *Merocystis kathae*. Phylogenomic analyses show that these taxa, together with *Rhytidocystis*, form a new lineage of apicomplexans that is sister to the Coccidia and Hematozoa (the lineages including most medically significant taxa). Members of this clade retain plastid genomes and the canonical apicomplexan plastid metabolism. However, the apicoplast genomes of *Margolisiella* and *Rhytidocystis* are the most reduced of any apicoplast, are extremely GC-poor, and have even lost genes for the canonical plastidial RNA polymerase. This new lineage of apicomplexans, for which we propose the class Marosporida *class nov.*, occupies a key intermediate position in the apicomplexan phylogeny, and adds a new complexity to the models of stepwise reductive evolution of genome structure and organelle function in these parasites.

Key words: organelle evolution, plastids, apicomplexans, phylogenomics.

Significance

Apicomplexans are obligate parasites of animals, however, they evolved from algae and retain a nonphotosynthetic plastid (the apicoplast). Using phylogenomics, we resolve the branching order of major apicomplexan lineages, and identify a new class of apicomplexans, the Marosporida. We also show marosporidians have the most reduced apicoplast genomes sequenced to date, which lack canonical plastidial RNA polymerase and provide new insights into reductive organelle evolution.

Introduction

The Apicomplexa is a phylum of obligate animal parasites including agents of significant human disease such as malaria (*Plasmodium* spp.) and toxoplasmosis (*Toxoplasma gondii*), and core symbionts of corals (Seeber et al. 2013; Kwong et al. 2019). They are abundant parasites in nature, with over 6,000 species described and thousands more likely yet to be discovered (Votýpka et al. 2017). Apicomplexan-like parasitism has arisen at least four times in parallel from a free-living plastid-bearing ancestor (Janouškovec et al. 2019; Mathur et al. 2019). In each case, the parasite morphology has converged around the use of an ancestral "apical complex" structure, which was originally used for feeding but was coopted for infection (Dos Santos Pacheco et al. 2020). Likewise, during each transition to parasitism, the chloroplast underwent convergent reduction, giving rise to a reduced, nonphotosynthetic chloroplast, known as the apicoplast. Since its surprising discovery (McFadden et al. 1996; Wilson et al. 1996), the apicoplast has been thoroughly investigated as a potential drug target for apicomplexan diseases, and for clues into the evolutionary origins of apicomplexans (Ralph et al. 2001). This reduced organelle is responsible for the essential biosynthesis of isoprenoids, fatty acids, and iron–sulfur clusters (Lim and McFadden 2010). Although the evolutionary origin of the apicoplast was previously contentious (Keeling 2010), it is now known to be a secondary, red-algal derived plastid that shares a common ancestor with the peridinin-containing plastids found in the sister group to apicomplexans, the dinoflagellates (Janouškovec et al. 2010).

The apicoplast genome is highly reduced, and has become a model for genome evolution in cryptic organelles. Across apicomplexan lineages, the gene content of apicoplasts has proven to be remarkably conserved: they have lost all genes encoding proteins that function directly in photosynthetic electron transfer (i.e., photosynthesis-related genes), they retain genes of nonphotosynthetic function, and their genomes are thought to be maintained due to the retention of a small number of nonhousekeeping genes (Janouškovec et al. 2010). One major exception is the recently described corallicolids (coral symbionts) whose plastids contain four genes involved in chlorophyll biosynthesis in addition to the traditional gene repertoire (Kwong et al. 2019). Phylogenies of plastid-encoded proteins place the corallicolids at the base of the Apicomplexa, which suggests that this may be an ancestral state that was simply lost early in other apicomplexan lineages. In contrast, the nuclear small subunit rRNA gene and mitochondrial phylogenies place the corallicolids closer to the Coccidia, suggesting a more complex history of apicoplast gene loss. A similar incongruence between plastid and nuclear phylogenies was recently observed in the mutualistic apicomplexan, *Nephromyces* (Muñoz-Gómez et al. 2019), and both studies suggested that the currently poor sampling of plastid data from deep-branching and diverse apicomplexan lineages may be a reason for conflicting phylogenetic signals.

To gain further insights into the evolutionary history of the apicoplast, and plastid evolution more generally, we performed whole-genome shotgun (WGS) and transcriptome sequencing surveys on three understudied, deep-branching apicomplexan species, *Aggregata octopiana*, *Merocystis kathae*, and *Margolisiella islandica*. Using phylogenomics, we present a robust multigene apicomplexan phylogeny incorporating all published apicomplexan taxa to date (Janouškovec et al. 2019; Mathur et al. 2019; Muñoz-Gómez et al. 2019). We show that species of the genera *Aggregata*, *Merocystis*, *Margolisiella*, together with *Rhytidocystis*, are part of a previously unrecognized, monophyletic group of marine invertebrate-infecting apicomplexans that is sister to the Haemosporidia, Piroplasmida, and Coccidia. We also reconstruct the complete apicoplast genomes and plastid metabolism of all three species, in addition to that of four other deep-branching apicomplexan species, *Siedleckia nematoides*, *Eleutheroschizon duboscqi*, *Rhytidocystis* sp. 1, and *Rhytidocystis* sp. 2. We find that the apicoplasts of *Aggregata*, *Merocystis*, *Siedleckia*, and *Eleutheroschizon* closely resemble other known apicomplexans in gene content and structure. However, the apicoplast genomes of *Margolisiella* and *Rhytidocystis* spp. differ from all known apicoplasts, in that they are more severely reduced, divergent, and have lost the highly conserved plastid-encoded RNA polymerase (rpoBC) operon.

Results and Discussion

A Resolved Multiprotein Phylogeny of the Apicomplexa

We generated new transcriptomes and WGS sequencing data for *M. kathae* and *Ma. islandica*, and WGS data from *A. octopiana*, after isolating the parasites from their marine mollusc hosts (SRA PRJNA645464). *Margolisiella islandica* is known to infect Icelandic scallops (*Chlamys islandica*) where it causes an intracellular infection in the heart auricle (Kristmundsson et al. 2011), *A. octopiana* primarily infects the gastrointestinal tract of the common octopus (*Octopus vulgaris*) with various intermediate crustacean hosts (Gestal et al. 1999; Castellanos-Martínez et al. 2013, 2019), and *M. kathae* infects the renal tissues of the common whelk (*Buccinum undatum*) with intermediate life stages in scallops (Kristmundsson and Freeman 2018) (fig. 1*Aa–c*). Host tissue infected with oocysts were dissected and washed to isolate parasite sporocysts and sporozoites from which RNA and DNA were extracted and sequenced for transcriptome and WGS analysis.

To place these species within a phylogenomic context, we added them to a data set of slow-evolving nuclear genes previously used to resolve deep phylogenetic relationships within the Apicomplexa (Mathur et al. 2019). This data set
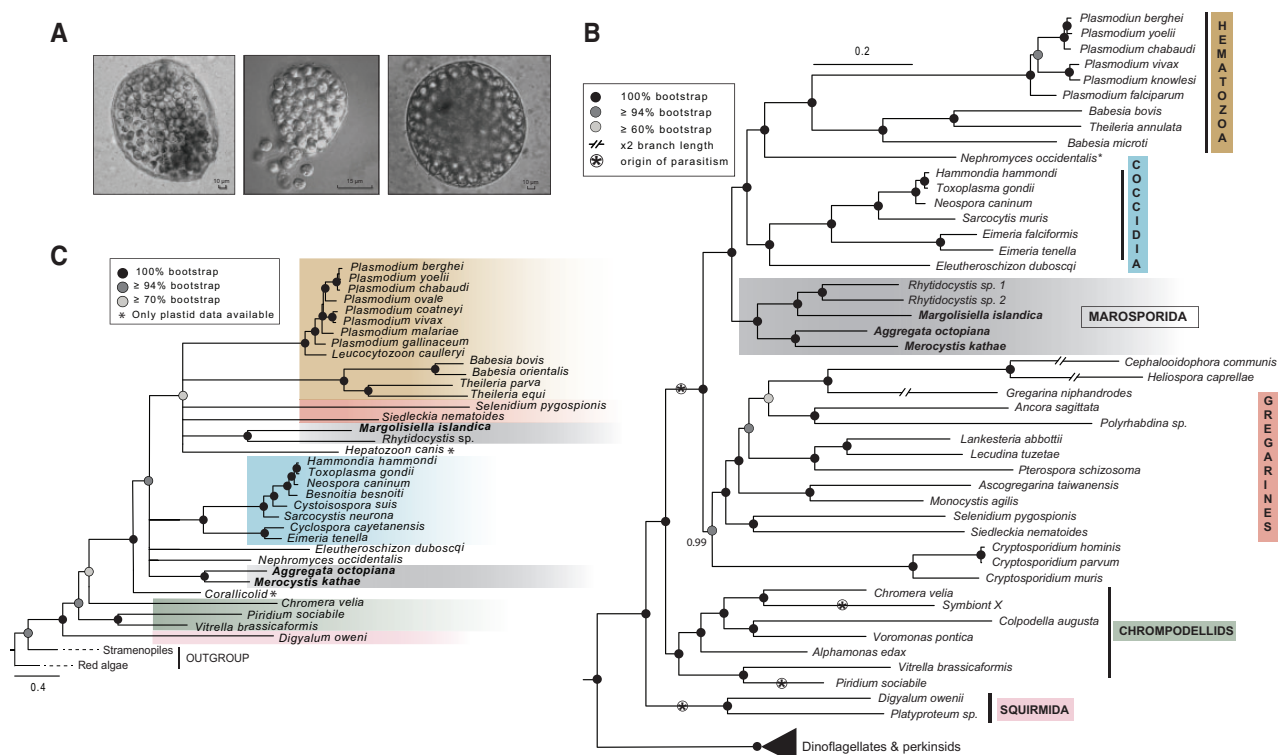
FIG. 1.—Phylogeny of the Apicomplexa. (*A*) Light micrographs of oocysts of the species sequenced, left to right, *Merocystis kathae*, *Margolisiella islandica*, and *Aggregata octopiana*. Scale bars are indicated on the figure. (*B*) A maximum-likelihood tree of apicomplexans and their relatives based on 195 nucleus-encoded protein markers and 58,611 amino acid sites. Newly sequenced species from this study are shown in bold. Circles at the nodes correspond to nonparametric bootstrap support (1,000 replicates, LG+F+G4 model) and Bayesian posterior probabilities (PP) (PhyloBayes, consensus of two independent chains, GTR+CAT model). All nodes shown have a PP of 1 unless otherwise indicated. The list of proteins used in the phylogenetic matrix, missing data proportions, and the BUSCO completeness of the newly sequenced species can be found in supplementary table S1, Supplementary Material online. * denotes that *Nephromyces* is a chimeric OTU assembled from several most closely related lineages from inside the renal sac of a single host. (*C*) A maximum-likelihood tree of apicomplexans based on 22 plastid-encoded genes and 5,759 amino acid sites. Branch support values are inferred from 500 nonparametric bootstraps (IQ-TREE model LG+F+R7) and are indicated by shaded circles on the nodes. Nodes with support <70% have been collapsed into polytomies. The shading corresponds to the groupings colored in figure 1A. * denotes taxa that only have plastid genome data available.

was also expanded to incorporate 11 other recently published transcriptomes (Janouškovec et al. 2019; Muñoz-Gómez et al. 2019). The final phylogenetic matrix included 55 taxa, 194 conserved, nucleus-encoded genes, and 58,611 amino acid sites (supplementary table S1, Supplementary Material online). Maximum-likelihood phylogenies using an empirical profile mixture model (LG+C40+F+G4), and Bayesian analyses using the CAT-GTR model (chain bipartition discrepancies: max diff. = 0.017) (Lartillot et al. 2009; Stamatakis 2014) produced congruent topologies that were well resolved and statistically supported at most internal nodes (fig. 1B). The resulting phylogenomic tree confirms the polyphyletic distribution of apicomplexan parasitism, with at least four origins. *Digyalum* is robustly sister to *Platyproteum*, together forming the "Squirmida" (Cavalier-Smith 2014), a group sister to all apicomplexans and chrompodellids (chromerids and colpodellids). *Nephromyces* is sister to the hematozoa (Muñoz-Gómez et al. 2019) and the gregarines (eugregarines and

archigregarines) form a fully-supported monophyletic group. The position of *Cryptosporidium* remains problematic: in these analyses, it is recovered as sister to the gregarines, but with somewhat weaker support.

A New Apicomplexan Class, Marosporida, That Infects Marine Invertebrates

Aggregata, *Merocystis*, and *Margolisiella* all branch with *Rhytidocystis* in a robustly supported monophyletic group (fig. 1B). The recovery of *Aggregata* and *Merocystis* as sister taxa is congruent with traditional taxonomic studies and 18S rRNA small subunit gene phylogenies, which have led to their placement in the family, Aggregatidae (Patten 1935; Kristmundsson and Freeman 2018) (supplementary fig. S1, Supplementary Material online). However, the Aggregatidae has been placed within the Coccidia, which is not consistent with the phylogenomic tree (fig. 1B). Similarly, the placement

of *Margolisiella* as the sister taxon to *Rhytidocystis* has also been observed previously in rRNA phylogenies, although with variable statistical support (Kristmundsson et al. 2011; Miroliubova et al. 2020) (supplementary fig. S1, Supplementary Material online). Historically, however, *Rhytidocystis* and *Margolisiella* have typically been classified into separate coccidian families, Agamococcidiorida and Eimeriidae, respectively (Levine 1979; Desser and Bower 1997; Leander and Ramey 2006), and very recently proposed to be a new subgroup, Eococcidia, based on concatenated rRNA operon phylogeny, which did not include *Aggregata* or *Merocystis* (Miroliubova et al. 2020). Here, we show with robust multiprotein phylogenomics that these taxa are sisters, but are not coccidians (fig. 1*B*).
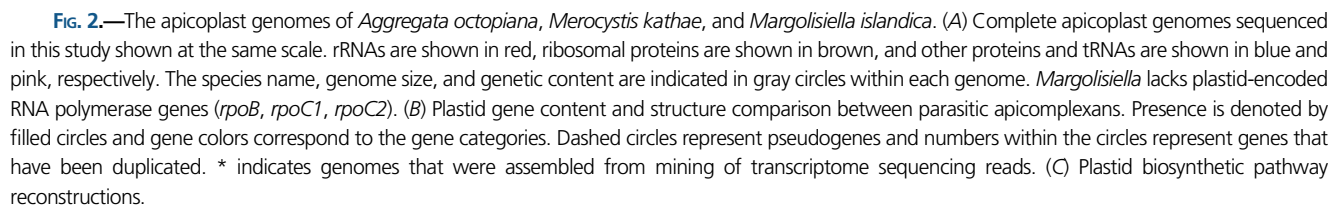
The past taxonomic treatments of all these organisms are complex and contradictory. Indeed, the entire apicomplexan lineage is in need of a major revision to better reflect conclusions from molecular and phylogenomic analyses. To best represent their relationships and avoid the confusion of names representing contradictory taxonomic proposals, we propose a new apicomplexan Class, Marosporida, named to reflect the marine nature of the currently recognized members. Within this group, we propose existing subgroups that do not contradict the phylogenetic relationships can be retained: the Aggregatidae is therefore transferred from the Coccidia to the Marosporida to reflect the sister relationship of *Aggregata* and Merocystis, and similarly the Rhytidocystidae, which was erected for the genus *Rhytidocystis* (Levine 1979; Leander and Ramey 2006; Rueckert and Leander 2009), can also be transferred to the Marosporida. The Eococcidia (Miroliubova et al. 2020) is also consistent with current phylogenomics, and could be transferred to the Marosporida, although it carries with it the potentially misleading reference to Coccidia. The Agamococcidiorida is an extremely problematic group that will need to be revisited and perhaps abandoned. This group originally contained Rhytidocystidae and Gemmocystidae, which included one member: *Gemmocysitis cylindrus*, a coral-infecting species that was suggested from histology to be closely related to *Rhytidocystis* (Upton and Peters 1986). *Gemmocystis* is now often hypothesized to be related to a broader group of coral-infecting apicomplexans, the corallicolids (Kwong et al. 2019). This cannot be tested with molecular data since none was produced for *Gemmocystis*, but we can conclude that corallicolids are not related to Rhytidocystidae (Kwong et al. 2019; Miroliubova et al. 2020). Whether the corallicolids are also members of Marosporida is still an open question. Corallicolid transcriptomic data remain unavailable, however, 18S rRNA and mitochondrial gene phylogenies do not support this grouping (supplementary figs. S1 and S2, Supplementary Material online; Miroliubova et al. 2020), which, together with the lack of data from other key taxa like *Pseudoklossia* and *Adelina*,

highlight the need for comparable sequencing data from additional apicomplexan lineages.

Taxon Sampling Does Not Improve Congruence between Apicoplast and Nuclear Phylogenies

Strongly conflicting signals between apicoplast-encoded and nuclear gene phylogenies have been observed in recent publications (Kwong et al. 2019; Muñoz-Gómez et al. 2019), which is unexpected given their shared evolutionary history. One explanation for the incongruence is that deep-branching apicoplast genomes are poorly sampled, making phylogenetic reconstructions less reliable. To fill this gap, we reanalyzed the apicoplast phylogeny with significantly greater taxonomic diversity. To obtain apicoplast genomes from *Aggregata*, *Merocystis*, and *Margolisiella*, we conducted WGS sequencing using DNA from parasite sporocysts isolated directly from host tissue. In addition, we also assembled a number of complete or near-complete apicoplasts from other previously reported transcriptome data that contained plastid genes, including those of *Rhytidocystis* sp. 1, *Rhytidocystis* sp. 2, *Eleutheroschizon*, *Siedleckia*, *Selenidium*, and *Digyalum* (Janouškovec et al. 2019). We used hidden Markov models (HMMs) to comprehensively search these transcriptomes for 40 apicoplast-encoded proteins using alignments curated for plastid phylogenomic analyses (Mathur et al. 2019). Apicoplast-encoded protein sequences were filtered and concatenated resulting in a phylogenetic matrix consisting of 58 taxa, 22 proteins, and 5,759 amino acid sites (supplementary table S2, Supplementary Material online). Using this matrix in combination with ML and Bayesian phylogenetic analyses, we recovered a poorly resolved phylogeny (fig. 1*C*).

The plastid phylogeny, even with the addition of 10 new deep-branching apicomplexans, remains poorly supported and incongruent with the nuclear phylogeny, specifically with respect to the branching order of the major groups (fig. 1*C*). Both phylogenies fully support the sister relationships between *Merocystis* and *Aggregata*, and *Margolisiella* and *Rhytidocystis*. The plastid phylogeny also recovers a monophyletic grouping of the Hematozoa, Piroplasmida, and Coccidia. However, the positions of the gregarines, *Selenidium* and *Siedleckia*, as well as *Nephromyces*, *Hepatozoon*, and *Eleutheroschizon* are not resolved. Interestingly, the position of corallicolids as the sister to all other apicomplexans in the plastid phylogeny is fully supported in agreement with previous analyses with less diversity (Kwong et al. 2019). The phylogeny was repeated excluding plastid genes extracted from transcriptome data (supplementary fig. S3, Supplementary Material online), which did not improve the support. We also progressively removed fast-evolving sites from the phylogenomic matrix, and tested the stability of the poorly supported nodes (supplementary fig. S4, Supplementary Material online). The node placing *Aggregata* and *Merocystis* sister to all apicomplexans other than corallicolids,

FIG. 2.—The apicoplast genomes of *Aggregata octopiana*, *Merocystis kathae*, and *Margolisiella islandica*. (A) Complete apicoplast genomes sequenced in this study shown at the same scale. rRNAs are shown in red, ribosomal proteins are shown in brown, and other proteins and tRNAs are shown in blue and pink, respectively. The species name, genome size, and genetic content are indicated in gray circles within each genome. *Margolisiella* lacks plastid-encoded RNA polymerase genes (*rpoB*, *rpoC1*, *rpoC2*). (B) Plastid gene content and structure comparison between parasitic apicomplexans. Presence is denoted by filled circles and gene colors correspond to the gene categories. Dashed circles represent pseudogenes and numbers within the circles represent genes that have been duplicated. * indicates genomes that were assembled from mining of transcriptome sequencing reads. (C) Plastid biosynthetic pathway reconstructions.

remains stable, as does support for *Eleutheroschizon* branching basal to the Coccidia (which is also consistent with its position in the nuclear topology). All other deep nodes with poor support have low and fluctuating bootstrap support with the progressive removal of fast-evolving sites indicative of phylogenetic artifacts. Overall, the significant augmentation of apicoplast diversity does little to resolve the incongruence between plastid and nuclear gene trees. Given the fast-evolving nature of the extremely AT%-rich apicoplast genomes, together with the fact that far fewer genes are available in the plastid genome for phylogenomic analyses

(5,759 sites in the plastid tree compared with 58,611 sites in the nuclear tree), we conclude, in agreement with the findings of Muñoz-Gómez et al. (2019), that the apicoplast-based analyses are less robust in resolving phylogenetic relationships within the Apicomplexa.

Apicoplast Genomes in *Margolisiella* and *Rhytidocystis* Are Highly Reduced and Lack RNA Polymerase Genes

The *Aggregata* and *Merocystis* apicoplast genomes are extremely similar in gene content, synteny, and size (fig. 2A).

They contain compact (∼38 kb) circular-mapping genomes with an inverted repeat including the 5S, 16S, and 23S rRNAs and the ribosomal protein gene *rps4*, like apicoplasts of Coccidia and corallicolids. They lack all genes involved in photosynthesis, including the four chlorophyll biosynthesis genes found in the corallicolids (*chlL*, *chlN*, *chlB*, and *acsF*). The only significant differences between the two genomes are the presence of the ribosomal protein gene *rpl11* and the RNA polymerase (RNAP) subunit *rpoC2A* being split in two open reading frames in *Merocystis* but not *Aggregata*. Therefore, their apicoplast genomes are overall extremely similar to each other in both structure and gene content, and do not differ substantially from the apicoplast genomes found in the Coccidia and Haemosporidia (fig. 2B).

Unlike *Merocystis* and *Aggregata*, the plastid genome of *Margolisiella* is strikingly reduced compared with all other apicoplasts sequenced to date (fig. 2A and B). The genome is very small (18 kb), with a strong AT% bias (13.3% GC). The genome is circular, extremely compact, and contains a single copy of the 16S and 23S rRNA genes, and a reduced complement of 18 tRNA genes and 13 ribosomal proteins, along with a single copy of the *tufA*, *clpC*, and *sufB* proteins, three ribosomal protein pseudogenes, and two hypothetical proteins (fig. 2A and B). *Margolisiella* also uses an alternate genetic code where UGA (the "opal" stop codon in the standard genetic code) encodes tryptophan, which is also found in the corallicolids, *Nephromyces*, and the two chrompodellids, *Piridium* and *Chromera* (Janouškovec et al. 2010; Kwong et al. 2019; Mathur et al. 2019; Muñoz-Gómez et al. 2019). Unlike all other known apicoplasts, the *Margolisiella* apicoplast genome has lost all four of its plastid-encoded RNAP genes, which are presumed to be solely responsible for the transcription of the apicoplast genome and therefore are functionally indispensable (Nisbet and McKenzie 2016).

A similarly AT-rich fraction of sequence reads was also observed by Janouškovec et al. (2019) in two species of *Rhytidocystis*, where the authors found apicoplast proteins in their transcriptome data. Organellar genomes with their high copy number and elevated expression levels can be highly represented not only in genome sequences but also in transcriptomes if their AT-rich transcripts are enriched by the poly-A selection step (Smith 2013). To determine whether the rhytidocystid apicoplast genomes resembled that of *Margolisiella*, we mined the publicly available transcriptomes from *Rhytidocystis* sp. 1 (which infects *Travisia forbesii*) and *Rhytidocystis* sp. 2 (which infects *Ophelia limacina*), for plastid sequences and were able to assemble complete apicoplast genomes. These searches also revealed numerous plastid contigs that allowed for the assembly of complete circular genomes from *S. nematoides* and *E. duboscqi* (supplementary fig. S5, Supplementary Material online) and fragmented genomic contigs that included most of the expected genes from *Selenidium* and *Digyalum* (see Materials and Methods) (supplementary table S2, Supplementary Material online).

The *Rhytidocystis* apicoplast genomes are even more reduced than *Margolisiella* (13 and 14 kb, in *Rhytidocystis* sp. 1 and sp. 2, respectively). They are extraordinarily AT-rich, with a GC content of 11.6% in *Rhytidocystis* sp. 1, and 9% in *Rhytidocystis* sp. 2. These are the most AT-rich plastid genomes sequenced to date, and *Rhytidocystis* sp. 2 even surpasses the AT-richness of the holoparasitic plant, *Balanophora* (Su et al. 2019). Although the two species are in the same genus, their apicoplast genomes show considerable divergence. *Rhytidocystis* sp. 1 is more reduced, and encodes only six ribosomal proteins, the 16S and 23S rRNAs, 4 tRNAs, *clpC* and *sufB*, whereas *Rhytidocystis* sp. 2 encodes seven ribosomal proteins (in addition to three that are pseudogenized), the 16S and 23S rRNAs, nine tRNAs, *clpC*, and *sufB* (fig. 2B). Strangely, *Rhytidocystis* sp. 1 uses an alternate genetic code (UGA encodes tryptophan), but *Rhytidocystis* sp. 2 uses the standard genetic code (fig. 2B). Both genomes lack all genes for RNAP, but interestingly have also lost the translation elongation factor, *tufA*, which is present in all other apicoplast genomes sequenced to date. The extreme compaction of the *Rhytidocystis* and *Margolisiella* apicoplast genomes demonstrates that genome reduction has not reached an "end point" in the majority of apicoplasts, despite the appearance of little variation from the best-studied groups, and further emphasizes the likely importance of only two genes, *sufB* and *clpC*, as a barrier to outright loss of the apicoplast genome (Janouškovec et al. 2015).

The Enigmatic Transcription of *Margolisiella* and *Rhytidocystis* Plastid Genes

The lack of plastid-encoded RNAPs in *Margolisiella* and *Rhytidocystis* raises the question of how their apicoplast genes are transcribed. We first explored the possibility that the RNAP genes had been transferred to the nucleus and that the plastid-derived polymerase proteins are imported back to the organelle, as many other plastid proteins are, and dinoflagellate plastid RNAPs are (Mungpakdee et al. 2014). We used a combination of BLAST and HMMs (Altschul et al. 1990; Finn et al. 2011) to comprehensively search for RNAP proteins based on domain structure and sequence composition in *Margolisiella* transcriptome and WGS data, and *Rhytidocystis* transcriptomes, but found no homologs, despite identifying plastid-encoded polymerase proteins (*rpoB* and *rpoC*) in all other apicoplast-bearing apicomplexans (fig. 3A). By comparison, we also searched for the "missing" *tufA* protein in *Rhytidocystis*, and found *tufA* transcripts from both species with canonical plastid targeting leaders, indicating that *tufA* has been transferred to the nucleus and that its protein product is targeted back to the apicoplast.

Another possible explanation, for which there is a precedent, is that the ancestral plastid-derived RNAP has been lost entirely, and apicoplast transcription relies on a separate and distinct nuclear-encoded polymerase derived from some other
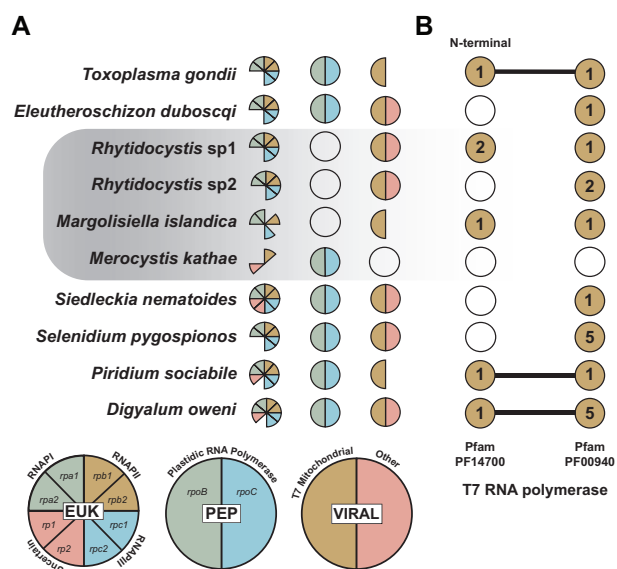
FIG. 3.—The RNA polymerases (RNAPs) present in plastid-bearing apicomplexans, *Digyalum* and *Piridium*. (A) The presence of eukaryotic RNAPs I, II, and III and other RNAPs with uncertain phylogenetic association, plastid-encoded RNA polymerases (PEP), and viral RNA polymerases are represented as portions of the circles. Empty circles indicate that no proteins were found. (B) The two domains of the bacteriophage-derived T7 polymerase (mitochondrial) are represented by circles. A line joining the circles signifies a complete T7 polymerase where the N-terminal domain is attached to the rest of the protein, and no line indicates fragmented proteins. Numbers within the circles denote the number of unique proteins identified.

source. Land plant plastids, for example, use two different RNAPs: a nuclear-encoded polymerase related to homologs from T7 bacteriophage that transcribes nonphotosynthesis genes, and the ancestral plastid polymerase that transcribes photosynthesis-related genes (Liere et al. 2011). Intriguingly, some holoparasitic plants that have lost many or all photosynthesis-related genes have also lost their functional plastid-encoded RNAP, and in the genus *Cuscata*, it has been demonstrated that all transcription is now carried out by the phage-derived polymerase (Krause et al. 2003; Krause 2008). To see if such an alternative polymerase exists in *Margolisiella* and *Rhytidocystis*, we searched their transcriptomes as well as the predicted proteins of other plastid-bearing apicomplexans with Pfam HMMs and identified all proteins containing domains associated with the two largest RNAP subunits, phage-type RNAPs, and other viral RNAPs (El-Gebali et al. 2018) (fig. 3A). We identified subunits of the eukaryotic RNA polymerases (RNAPI, II, and III) in all the apicomplexans searched, as well as a few phylogenetically ambiguous proteins that were not associated distinctly with a certain polymerase (labeled as "uncertain") (fig. 3A).

These searches also found T7 bacteriophage derived RNAPs in all taxa, except for *Merocystis* (fig. 3A), which may be due to the incompleteness of the *Merocystis* transcriptome

(refer to supplementary table S1, Supplementary Material online, for BUSCO completeness scores). Most eukaryotic mitochondria use a T7 phage polymerase for transcription of mitochondrial genes, and such polymerases have been found in the genomes of both dinoflagellates and apicomplexans (Li et al. 2001; Teng et al. 2013). All T7 polymerases that we recovered were found to be homologous to these mitochondrially targeted polymerases. In *Selenidium*, *Siedleckia*, and *Eleutheroschizon* we retrieved truncated proteins that lack the complete N-terminal domain, whereas in *Toxoplasma*, *Piridium*, and *Digyalum*, we recovered the complete protein (fig. 3B). Intriguingly, we found additional T7 polymerases in several apicomplexans, including *Rhytidocystis*. Two N-terminal domain fragments were found in *Rhytidocystis* sp. 1, whereas in *Rhytidocystis* sp. 2, we found two truncated T7 polymerase transcripts that are missing the N-terminal domain (fig. 3B). *Margolisiella* contained two nonoverlapping T7 polymerase fragments, but it was not clear if they are part of one protein or two different proteins. It is possible that a T7 phage-derived polymerase might be targeted to the apicoplast, or even that the mitochondrial T7 polymerase is dually targeted in these nonmodel species. A precedent comes from land plants, where a dually targeted RNAP with an ambiguous targeting sequence allows a mitochondrial T7 polymerase to be imported into both the chloroplast and the mitochondria (Hedtke et al. 2000). Another possibility is that mitochondrial T7 polymerase may contain a "twin" targeting sequence, represented by a mitochondrial and a chloroplast targeting sequence in tandem. This is seen in the protoporphyrinogen oxidase II enzyme in spinach, which has two in-frame initiation codons, and thus two different proteins are made by alternative translation where the longer protein is targeted to the chloroplasts and the shorter one to the mitochondria (Watanabe et al. 2001). Based on present sequencing data, we cannot convincingly identify the protein responsible for transcription of the *Margolisiella* and *Rhytidocystis* apicoplast-encoded genes, but we hypothesize that an unrecognized but ancient redundancy in apicomplexan RNAPs exists and that some single-subunit polymerase, such as a T7 phage polymerase, is targeted to these apicoplasts.

The Canonical Apicoplast Biosynthetic Function Is Conserved in Marosporida

Given the variability in apicoplast genomes in Marosporida, we explored the diversity of organelle function in *Aggregata*, *Merocystis*, and *Margolisiella*. Generally, apicoplasts are involved in biosynthesis of isoprenoids (MEP), fatty acids (FASII), iron–sulfur (Fe–S) clusters, and part of the tetrapyrrole (heme) biosynthesis pathway (Sheiner et al. 2013). Most apicomplexans retain genes for all four pathways, however, the piroplasms and "Symbiont-X" only carry out isoprenoid biosynthesis (Janouškovec et al. 2015, 2019), and the marine gregarine clade that includes *Pterospora*, *Lankesteria*, and

Lecudina only retain fatty acid biosynthesis (Mathur et al. 2019).

All plastid homologs for enzymes in these pathways were identified by HMM searches with previously curated alignments (Mathur et al. 2019; see Materials and Methods). We found evidence for the presence of all four pathways in the Marosporida (fig. 2C and supplementary table S3, Supplementary Material online). In *Margolisiella*, we found the complete fatty acid biosynthesis pathway, a near-complete Fe–S cluster assembly pathway, and homologs for several enzymes involved in both isoprenoid (*ispC, ispE, ispG*) and heme biosynthesis (*hemE* and *hemH*). In *Aggregata*, we found the complete isoprenoid biosynthesis and near-complete fatty acid pathway, as well as most enzymes involved in the Fe–S and heme pathways. We also found homologs from all pathways except the MEP pathway in *Merocystis*, however, none was complete, probably because the *Merocystis* transcriptomic data were not sequenced as deeply (refer to supplementary table S1, Supplementary Material online and fig. 2C for BUSCO completeness scores). We then searched for putative targeting leaders indicated by signal and transit peptides at the N-terminus of these plastid-targeted proteins using predictions from SignalP v5.0 and ChloroP v1.1 (Emanuelsson et al. 1999; Dyrløv Bendtsen et al. 2004). We found plastid targeting N-terminal signatures in 3 of these proteins (supplementary table S3, Supplementary Material online), including components of the Fe-S and FASII pathways. Interestingly, we also found evidence for the cytosolic type I fatty acid synthase in *Margolisiella* and *Aggregata*. This pathway has been lost in many apicomplexans, but is also retained in the Coccidia, suggesting that both Coccidia and Marosporida retain both type I (cytosolic) and type II (plastidic) fatty acid biosynthesis pathways (Mazumdar and Striepen 2007).

Summary and Future Directions

Here, we present a well-resolved phylogenetic framework of the Apicomplexa that includes nearly all recognized apicomplexan groups. This facilitated the identification of a new clade of diverse apicomplexans previously classified into several distinct subgroups, the Marosporida. Whole-genome shotgun and transcriptome sequencing shows that plastid metabolisms of this new group are conserved, but the apicoplast genome structure and content are highly variable. Apicoplasts from *Margolisiella* and *Rhytidocystis* have the smallest, most reduced, and most AT-biased genomes known to date, and have distinctively lost plastid-encoded RNAP genes. Taken together with the recent discovery of chlorophyll biosynthesis genes in corallicolids and the intragenus variation of the *Rhytidocystis* plastids, the patterns of gene retention and loss in deep-branching apicomplexans is more complex than previously thought, as are other relatively stable characters, such as noncanonical genetic codes. This variability will likely continue to increase with greater taxon sampling, given that we only have a handful of representatives from most lineages, and entirely lack complete apicoplast genomes from several key taxa, such as the archigregarines and squirmids. We also still lack nuclear genomic resources for several important groups, such as corallicolids and adeleids. Although our overall understanding of reductive plastid evolution and the emergence of parasitism in the Apicomplexa is still challenged by both gaps in taxon and subcellular compartment sampling, the unexpected genetic diversity and complex evolutionary patterns that have been revealed here and in other recent studies bring us closer to a comprehensive understanding of apicomplexan biology and evolution.

Taxa

Marosporida Mathur, Kristmundsson, Gestal, Freeman, and Keeling 2020

Definition: The phylogenetic clade containing *A. octopiana* Frenzel 1885 (Aggregatidae), *M. kathae* Dakin, 1911 (Aggregatidae), *Ma. islandica* (Kristmundsson et al. 2011), *Rhytidocystis* sp. 1 and *Rhytidocystis* sp. 2 (Rhytidocystidae) (Janouškovec et al. 2019).

Etymology: "Maro" refers to the marine environment that the hosts of these parasites inhabit.

Reference phylogeny: Figure 1, this paper. *Aggregata octopiana* is closely related to *M. kathae*, and *Ma. islandica* to *Rhytidocystis* sp. 1 and 2.

Comments: This clade is inferred from molecular phylogenies. This is a zoological name above level of order and as such falls outside the zoological (and botanical) codes of nomenclature.

Materials and Methods

Sample Collection and DNA/RNA Extraction

Merocystis kathae was isolated from a common whelk (*B. undatum*) and *Ma. islandica* was isolated from an Iceland scallop (*C. islandica*) that were collected by dredging in Breiðafjörður Bay, Iceland (65°7.576'N; 22°44.738'W). Prior to sampling, both the whelks and the scallops were sedated using 0.1% $MgSO_4$ in seawater for 1–2 h. The renal organ of the whelks was examined under a dissecting microscope for the presence of *Merocystis* infections. Subsequently, the relatively large gamogonic stages of *Merocystis* were retrieved by gently squeezing the renal organ with pointed forceps until the parasites were released. The resulting exudate was collected into concave glass spot plates containing filtered seawater and rinsed with autoclaved seawater three times to remove as much host tissues and mucous as possible. The auricles of the scallops were excised under a dissecting microscope, and infections of *Margolisiella* (all life stages present) examined from a small drop of hemolymph from the

auricles. Small samples from heavily infected heart auricles, and its hemolymph, were taken for molecular analysis. DNA and RNA from the samples, infected with *Merocystis* and *Margolisiella*, was extracted using a QIAGEN AllPrep DNA/RNA Mini Kit (Cat. No. 80204).

Aggregata octopiana was isolated from a pool of five infected octopuses (*O. vulgaris*) collected using traps by local fishermen in Ria de Vigo, Spain (24°14.09′N, 8°47.18′W).

Aggregata oocysts were observed as white spots on the digestive tract with light microscopy. The oocysts were extracted from the caecum and intestine, and light microscopy and histology were used to analyze the morphology and dimensions of the fresh sporocysts.

For DNA extraction, the digestive tract tissues infected with sporogonic stages of the parasite were dissected and homogenized in 10 ml of filtered seawater with 1% Tween 80 using an electric tissue grinder (IKA-Ultra Turrax T-25). Tissue homogenates were filtered twice with a nylon mesh of 100 and 41 μm, respectively, to remove tissue fragments. The filtrate was then centrifuged at $1,000 \times g$ for 5 min. The sporocysts were cleaned using a density gradient centrifugation method according to Gestal et al. (1999), and counted in a Neubauer chamber to standardize the sample at 2×10^6 sporocyst/ml. Light microscopy was used to analyze the morphology and dimensions of the fresh sporocysts. For DNA extraction, sporocysts were resuspended in 500 μl of extraction buffer (NaCl 100 mM, EDTA 25 mM pH 8, SDS 0.5%) and disrupted by wet bead milling using a Retsch Mixer Mill MM 300 grinder to release sporozoites. After Proteinase K (Sigma) digestion (1 mg ml^{-1}; 37 °C overnight), genomic DNA was purified using a phenol:chloroform:isoamil alcohol extraction method (Sambrook et al. 1989). DNA was precipitated with ethanol and sodium acetate overnight at −20 °C. The precipitated pellet was resuspended in 30 μl of sterile water.

Genome Sequencing, Plastid Genome Assembly, and Annotation

DNA samples from *A. octopiana*, *M. kathae*, and *Ma. islandica*, were prepared for WGS sequencing at The Centre for Applied Genomics in The Hospital for Sick Children using the Illumina TruSeq Nano kit. The resulting libraries were sequenced on the Illumina HiSeq X sequencer using 150-bp paired-end reads. All sequencing raw reads have been deposited under SRA PRJNA645464. The quality of the raw reads was assessed using FastQC and trimmed to remove sequencing adaptors with Trimmomatic v0.36 (Bolger et al. 2014; Andrews et al. 2015). Due to a high level of animal host contamination in the samples, the raw reads were first assembled with the metagenomic assembler, MEGAHIT v1.1.4-2 (Li et al. 2015). This initial assembly was used to search for apicoplast contigs using BLAST against known apicoplast genome sequences (Altschul et al. 1990). The raw reads were then mapped onto these apicoplast

contigs of interest and extracted using Bowtie v2.2.6 and BlobTools bamfilter (Laetsch and Blaxter 2017; Langmead et al. 2009). These extracted reads were used for the final apicoplast genome assemblies with Spades v3.11.1 (Bankevich et al. 2012). NOVOPlasty v2.6.3 was used to assemble the inverted repeat regions and close (circularize) the apicoplast genomes (Dierckxsens et al. 2016). The plastid genomes of *S. nematoides*, *Eleutheroschizon dubosqci*, and *Rhytidocystis* sp. 1 and sp. 2 were assembled by data mining publicly available RNA-Seq data. *Siedleckia* was assembled using NOVOPlasty v2.6.3, and *Eleutheroschizon* and *Rhytidocystis* were assembled based on contig overlaps from assemblies of raw transcript reads using rnaSPAdes 3.13.2 (Bushmanova et al. 2019). The apicoplast genomes were annotated manually in Geneious Prime (www.geneious.com/prime/) and ORFs larger than 100 amino acids were predicted, followed by BLAST searches against the NCBI GenBank non-redundant databases (Agarwala et al. 2018). rRNA genes were annotated based on predictions made by RNAmmer v1.2 using the "Bacteria" setting and tRNAs were annotated using tRNAscan-SE 2.0 (Lagesen et al. 2007; Chan and Lowe 2019).

Plastid Phylogenomic Analyses

A data set comprising 40 plastid-encoded proteins was compiled based on a previously published data set (Mathur et al. 2019) and enriched with all apicomplexan plastids that have been sequenced as of January 2020 (supplementary table S2, Supplementary Material online) as well as the plastid-encoded proteins of *A. octopiana*, *M. kathae*, and *Ma. islandica*. Profile HMMs searches with the above-mentioned protein alignments were also used to identify plastid-encoded proteins from transcriptomic data published by Janouškovec et al. (2019). Hits from the HMM search were aligned with MAFFT v7.222 and poorly aligned regions were removed using trimAl v.1.2 (-gt 0.8) (Capella-Gutierrez et al. 2009; Katoh and Standley 2013). Maximum-likelihood trees were made with FastTree v.2.1.7 using the default options (Price et al. 2010). The resulting phylogenies were inspected manually to remove contaminants and paralogs. The selected proteins were then added to the final protein alignments for phylogenomic analyses (see supplementary table S2, Supplementary Material online, for the list of taxa and proteins). The final protein alignments were aligned with MAFFT v7.222 using the –auto option and trimmed with trimAl v.1.2 (-gt 0.6) (Capella-Gutierrez et al. 2009; Katoh and Standley 2013). These alignments were then filtered so that they contained only a maximum of 26% missing OTUs and concatenated using SCaFoS v1.2.5 (Roure et al. 2007). The resulting concatenated alignment consists of 22 genes spanning 5,759 amino acid positions from 58 taxa (available at Mendeley data doi:10.17632/rrdc4xsk2h.1). The phylogenomic maximum-likelihood analyses were done in IQ-TREE

v.1.5.4 with the model LG+F+R7 and 500 nonparametric bootstraps. This model best fits the data according to the Akaike information criterion and the corrected Akaike information criterion as determined by ModelFinder (Kalyaanamoorthy et al. 2017). Fast evolving site removal was done using site rates generated in IQTREE v.1.5.4 (-wsr option) (Nguyen et al. 2015).

Transcriptome Sequencing and Assembly

Reverse transcription of RNA samples from *M. kathae* and *Ma. islandica* was carried out using the Smart-Seq2 protocol (Picelli et al. 2014). The cDNA concentration was quantified on a Qubit 2.0 Fluorometer (Thermo Fisher Scientific Inc.). Prior to high-throughput sequencing, 1 μl of the final cDNA product was used as a template for a PCR amplification of the V4 region of the 18S rRNA gene using Phusion High-Fidelity DNA Polymerase (New England Biolabs, Thermo Scientific) and the general eukaryotic primer pair TAReuk454FWD1 and TAReukREV3 (Stoeck et al. 2010). The PCR product was then sequenced by Sanger sequencing. The SSU rRNA gene sequences were used to confirm species specificity and avoid animal host contamination using BlastN to look for similar sequences in the nonredundant NCBI database (Johnson et al. 2008). Sequencing libraries were then prepared using the Nextera XT protocol, and sequenced on the Illumina MiSeq sequencer using 250-bp paired-end reads. All raw reads have been deposited under SRA PRJNA645464. The raw Illumina sequencing reads were merged using PEAR v0.9.6, and FastQC was used to assess the quality of the paired reads (Zhang et al. 2014; Andrews et al. 2015). The adapter and primer sequences were trimmed using Trimmomatic v0.36 and the transcriptomes was assembled with Trinity v2.4.0 (Grabherr et al. 2011; Bolger et al. 2014). The contigs were then filtered for animal host contamination using BlobTools in addition to BlastN and BlastX searches against the NCBI nt database and the SWISS-PROT database, respectively (Agarwala et al. 2018; Bateman 2019). Coding sequences were predicted using a combination of TransDecoder v3.0.1 and similarity searches against the SWISS-PROT database (Haas et al. 2013; Bateman 2019). The completeness of the transcriptomes were assessed with BUSCO v4.0.6 using the alveolate marker gene set (Simão et al. 2015) (supplementary table S1, Supplementary Material online).

Nuclear Phylogenomics Analyses

Transcriptome data from *M. kathae*, *Ma. islandica*, and recently published apicomplexan transcriptomes by Janouškovec et al. (SRA PRJNA557242) and Muñoz-Gómez et al. (SRR8618777) were added to our data set. The transcriptomes were searched using BlastP for a set of 263 genes that have been previously used for apicomplexan phylogenomic analyses and that represent a wide range of eukaryotes

(Altschul et al. 1990; Burki et al. 2016; Mathur et al. 2019). The hits were filtered using an e-value threshold of 1e-20 and a query coverage of 50%. In addition to this transcriptomic data set, the genomic reads of *A. octopiana* and *M. kathae* were also searched for the 263 genes using TBlastN with an e-value threshold of 1e-20. The complete regions of the contigs that contained hits were extracted and coding regions were predicted using Exonerate v.2.2.0 and TransDecoder-v5.1.0 (Slater and Birney 2005; Haas et al. 2013). The final 263 gene alignments were then aligned using MAFFT L-INS-i v7.222 and trimmed using trimAl v1.2 (-gt 0.8) (Capella-Gutiérrez et al. 2009; Katoh and Standley 2013). Single gene trees were then constructed to identify paralogs and contaminants using RAxML v8.2.12 (PROT-GAMMA-LG model) with support from 1,000 bootstraps (Stamatakis 2014) The resulting trees were manually viewed in FigTree v1.4.3 and contaminants and paralogous sequences were identified and removed (Rambaut 2014). The final cleaned gene-sets were filtered so that they contained only a maximum of 40% missing OTUs and then concatenated in SCaFoS v1.2.5 (Roure et al. 2007). The resulting concatenated alignment consisted of 194 genes spanning 58,611 amino acid positions from 54 taxa (available at Mendeley data doi:10.17632/rrdc4xsk2h.1). The phylogenomic maximum-likelihood tree was constructed with the heterogeneous mixture LG+C40+F+G4 model as implemented in IQ-TREE (Quang et al. 2008; Nguyen et al. 2015). Statistical support was inferred using 1,000 bootstrap replicates using the LG+F+G4 model in RAxML (Stamatakis 2014). The Bayesian tree was computed in PhyloBayes v4.1 using the GTR-CAT model with constant sites removed from the analyses (Lartillot et al. 2009). Four independent chains were run for 10,000 generations and two chains converged with max diff. = 0.017, whereas two chains got stuck at local maxima. However, all four chains recovered the same topology in regards to the support of the Marosporida clade with posterior probability of 1. Furthermore, the chains that recovered the same topology as the best tree had higher log likelihoods.

RNA Polymerase Analysis

To assess the presence and absence of RNAPs in *Margolisiella* and *Rhytidocystis* sp. 1 and sp. 2, we searched genomic and transcriptomic protein predictions from plastid bearing apicomplexans using PFAM HMMs ($E < 10^{-5}$, incE $< 10^{-5}$, domE $< 10^{-5}$) to identify proteins containing domains associated with the two largest RNAP subunits, Rpa1/Rpb1/Rpc1/RpoC (PF00623, PF04983, PF04990, PF04992, PF04997–PF05001), and Rpa2/Rpb2/Rpc2/RpoB (PF00562, PF04560, PF04561, PF04563, PF04565–PF04567, PF10385), as well as phage-type/mitochondrial RNAPs (PF00940, PF10385), and other viral RNAPs (PF00680, PF00978, PF00998, PF02123, PF07925, PF17501) (for a total of 24 PFAM domains) using HMMER v3.1 (Finn et al. 2011; El-Gebali et al. 2018) The same

searches were conducted against the SWISS-PROT database to identify nonapicomplexan outgroups (Bateman 2019). Identified SWISS-PROT and apicomplexan proteins were aligned using MAFFT v.7.222 using the PFAM seed alignments as references (Katoh and Standley 2013). The resulting alignments were then trimmed using trimAl v1.2 (-gt 0.3) before being used to generate maximum-likelihood phylogenies using FastTree v2.1.3 (Capella-Gutiérrez et al. 2009; Price et al. 2010). To identify which polymerase complexes these proteins corresponded to (e.g., eukaryotic RNAPI, RNAPII, RNAPIII, or prokaryotic RNAP), proteins were annotated using BlastP searches against the SWISS-PROT database (max_target_seqs 1, $E < 10^{-5}$) and their phylogenetic context was interpreted in FigTree. Phylogenetically ambiguous proteins that were not clearly associated with a certain polymerase were labeled as "uncertain."

Search for Plastid-Derived Biosynthetic Proteins

Profile HMMs were used to identify plastid metabolic proteins in our transcriptomes based on previously curated alignments (Mathur et al. 2019). Profile HMMs were generated using these alignments and HMM searches were conducted on all transcriptomes and genomes using HMMER v3.1 and an e-value threshold of 1e-5 (Finn et al. 2011). In addition to this transcriptomic data set, the WGS contigs of *Aggregata*, *Merocystis*, and *Margolisiella* were also searched for the plastid-targeted proteins using TBlastN with an e-value threshold of 1e-20. The complete regions of the contigs that contained hits were extracted and coding regions were predicted using Exonerate v.2.2.0 and TransDecoder-v5.1.0 (Slater and Birney 2005; Haas et al. 2013). All resulting hits were then extracted and incorporated into the original alignments and realigned using MAFFT v7.222 (–auto option). The alignments were then used to generate phylogenies in FastTree v2.1.3 (Price et al. 2010). The phylogenies were manually scanned in FigTree v1.4.2 and contaminants, paralogs, mitochondrial sequences, and long-branching divergent sequences were identified and removed (Rambaut 2014). The remaining sequences were realigned and used to generate maximum-likelihood phylogenies in IQ-TREE v.1.6.9 (Nguyen et al. 2015). Phylogenetic models were selected for each tree individually based on Bayesian Information Criteria using ModelFinder as implemented in IQ-TREE, and statistical support was assessed using 1,000 ultrafast bootstrap pseudoreplicates (Nguyen et al. 2015; Kalyaanamoorthy et al. 2017). SignalP v5.0 and ChloroP v1.1 were used to predict plastid targeting signals on the N-terminal in the proteins recovered (Emanuelsson et al. 1999; Dyrløv Bendtsen et al. 2004). Refer to supplementary table S3, Supplementary Material online, for all plastid-targeted proteins and localization signals recovered.

Mitochondrial and 18S Ribosomal Small Subunit Gene Phylogenies

The three mitochondria-encoded proteins, *cox1*, *cox3*, and *cob*, were extracted using BLAST searches against the transcriptomes and WGS assemblies (Altschul et al. 1990). Single protein alignments were generated using MAFFT v7.222 (–auto option) and trimmed using trimAl v1.2 (-gt 0.6) (Capella-Gutierrez et al. 2009; Katoh and Standley 2013). Proteins were concatenated in Geneious Prime v 2020.1.1. The phylogeny was constructed in IQ-TREE with the LG+F+I+G4 model and 1,000 ultrafast bootstraps. The best-fit model was chosen according to the Bayesian information criterion (BIC) using Model Finder (Kalyaanamoorthy et al. 2017). Nuclear 18S rRNA genes were extracted using BLAST searches against the transcriptomes and genomes (Altschul et al. 1990). Genes were aligned with MAFFT v7.222 (–auto option) and trimmed using trimAl v1.2 (-gt 0.6) (Capella-Gutierrez et al. 2009; Katoh and Standley 2013). Phylogenies were constructed in IQ-TREE with the GTR+G+I model and 1,000 ultrafast bootstraps.

Supplementary Material

Supplementary data are available at *Genome Biology and Evolution* online.

Author Contributions

V.M. and P.J.K. designed the study. A.K., M.F., and C.G. obtained samples. V.M. and F.H. performed transcriptomics and WGS preparation. V.M., F.H., and W.K.K. assembled and annotated the plastids. V.M. and N.A.T.I. carried out the RNAP analysis. V.M. analyzed the rest of the data. V.M. and P.J.K. wrote the paper with input from all authors.

Data Availability

The plastid genomes generated here are available at the NCBI GenBank Nucleotide Database (www.ncbi.nlm.nih.gov/nucleotide/) and can be accessed with the following accession numbers: MW088710, MW088711, and MW088712. The raw sequencing reads are available on the Sequence Read Archive (www.ncbi.nlm.nih.gov/sra/) and be accessed with the accession PRJNA645464. The alignments for the phylogenomics analyses and transcriptome-mined plastid genomes are available at Mendeley Data (www.mendeley.com/datasets) and can be accessed with the doi:10.17632/rrdc4xsk2h.3.

Literature Cited

Agarwala R, et al. 2018. Database resources of the National Center for Biotechnology Information. Nucleic Acids Res. 46:D8–D13.

Altschul SF, Gish W, Miller W, Myers EW, Lipman DJ. 1990. Basic local alignment search tool. J Mol Biol. 215(3):403–410.

Andrews S, Krueger F, Seconds-Pichon A, Biggins F, Wingett S. 2015. FastQC. A quality control tool for high throughput sequence data. Babraham Bioinformatics. Babraham Inst. [Internet] 1:1. Available from: https://www.bioinformatics.babraham.ac.uk/projects/fastqc/

Bankevich A, et al. 2012. SPAdes: a new genome assembly algorithm and its applications to single-cell sequencing. J Comput Biol. 19(5):455–477.

Bateman A. 2019. UniProt: a worldwide hub of protein knowledge. Nucleic Acids Res. 47:D506–D515.

Bolger AM, Lohse M, Usadel B. 2014. Trimmomatic: a flexible trimmer for Illumina sequence data. Bioinformatics 30(15):2114–2120.

Burki F, et al. 2016. Untangling the early diversification of eukaryotes: a phylogenomic study of the evolutionary origins of Centrohelida, Haptophyta and Cryptista. Proc R Soc B. 283(1823):20152802. doi:10.1098/rspb.2015.2802.

Bushmanova E, Antipov D, Lapidus A, Prjibelski AD. 2019. rnaSPAdes: a de novo transcriptome assembler and its application to RNA-Seq data. GigaScience 8(9):giz100. doi:10.1093/gigascience/giz100.

Capella-Gutierrez S, Silla-Martinez JM, Gabaldon T. 2009. trimAl: a tool for automated alignment trimming in large-scale phylogenetic analyses. Bioinformatics 25(15):1972–1973.

Castellanos-Martínez S, Gestal C, Pascual S, Mladineo I, Azevedo C. 2019. Protist (Coccidia) and Related Diseases. In: Gestal C, Pascual S, Guerra Á, Fiorito G, Vieites J, editors. Handbook of Pathogens and Diseases in Cephalopods. Cham: Springer. 10.1007/978-3-030-11330-8_9

Castellanos-Martínez S, Pérez-Losada M, Gestal C. 2013. Molecular phylogenetic analysis of the coccidian cephalopod parasites Aggregata octopiana and Aggregata eberthi (Apicomplexa: Aggregatidae) from the NE Atlantic coast using 18S rRNA sequences. Eur J Protistol. 49(3):373–380.

Cavalier-Smith T. 2014. Gregarine site-heterogeneous 18S rDNA trees, revision of gregarine higher classification, and the evolutionary diversification of Sporozoa. Eur J Protistol. 50(5):472–495.

Chan PP, Lowe TM. 2019. tRNAscan-SE: Searching for tRNA genes in genomic sequences. In: Methods in Molecular Biology. Vol. 1962. New York:Humana Press Inc. p. 1–14.

Desser SS, Bower SM. 1997. Margolisiella kabatai gen. et sp. n. (Apicomplexa: Eimeriidae), a parasite of native littleneck clams, Protothaca staminea, from British Columbia, Canada, with a taxonomic revision of the coccidian parasites of bivalves (Mollusca: Bivalvia). Folia Parasitol (Praha). 44:241–247.

Dierckxsens N, Mardulyn P, Smits G. 2016. NOVOPlasty: de novo assembly of organelle genomes from whole genome data. Nucleic Acids Res. 45:gkw955.

Dos Santos Pacheco N, Tosetti N, Koreny L, Waller RF, Soldati-Favre D. 2020. Evolution, composition, assembly, and function of the conoid in Apicomplexa. Trends Parasitol. 36(8):688–704.

Dyrløv Bendtsen J, Nielsen H, von Heijne G, Brunak S. 2004. Improved prediction of signal peptides: signalP 3.0. J Mol Biol. 340(4):783–795.

El-Gebali S, et al. 2018. The Pfam protein families database in 2019. Nucleic Acids Res. 47:427–432.

Emanuelsson O, Nielsen H, Heijne GV. 1999. ChloroP, a neural network-based method for predicting chloroplast transit peptides and their cleavage sites. Protein Sci. 8(5):978–984.

Finn RD, Clements J, Eddy SR. 2011. HMMER web server: interactive sequence similarity searching. Nucleic Acids Res. 39(Suppl):W29–W37.

Gestal C, Abollo E, Pascual S. 1999. Evaluation of a method for isolation and purification of sporocysts of the cephalopod coccidian parasite Aggregata Frenzel, 1885 (Apicomplexa: Aggregatidae). Iberus Rev la Soc Española Malacol. 17:115–121.

Grabherr MG, et al. 2011. Full-length transcriptome assembly from RNA-Seq data without a reference genome. Nat Biotechnol. 29(7):644–652.

Haas BJ, et al. 2013. De novo transcript sequence reconstruction from RNA-seq using the Trinity platform for reference generation and analysis. Nat Protoc. 8(8):1494–1512.

Hedtke B, Börner T, Weihe A. 2000. One RNA polymerase serving two genomes. EMBO Rep. 1(5):435–440.

Janouškovec J, et al. 2015. Factors mediating plastid dependency and the origins of parasitism in apicomplexans and their close relatives. Proc Natl Acad Sci U S A. 112(33):10200–10207.

Janouškovec J, et al. 2019. Apicomplexan-like parasites are polyphyletic and widely but selectively dependent on cryptic plastid organelles. Elife 8:1–24.

Janouškovec J, Horak A, Obornik M, Lukes J, Keeling PJ. 2010. A common red algal origin of the apicomplexan, dinoflagellate, and heterokont plastids. Proc Natl Acad Sci U S A. 107(24):10949–10954.

.Johnson M, Zaretskaya I, Raytselis Y, Merezhuk Y, McGinnis S, Madden TL. 2008. NCBI BLAST: a better web interface. Nucleic Acids Res. [Internet] 36. Available from: 10.1093/nar/gkn201

Kalyaanamoorthy S, Minh BQ, Wong TKF, von Haeseler A, Jermiin LS. 2017. ModelFinder: fast model selection for accurate phylogenetic estimates. Nat Methods. 14(6):587–589.

Katoh K, Standley DM. 2013. MAFFT multiple sequence alignment software version 7: improvements in performance and usability. Mol Biol Evol. 30(4):772–780.

Keeling PJ. 2010. The endosymbiotic origin, diversification and fate of plastids. Philos Trans R Soc B. 365(1541):729–748.

Krause K. 2008. From chloroplasts to "cryptic" plastids: evolution of plastid genomes in parasitic plants. Curr Genet. 54(3):111–121.

Krause K, Berg S, Krupinska K. 2003. Plastid transcription in the holoparasitic plant genus Cuscuta: parallel loss of the rrn16 PEP-promoter and of the rpoA and rpoB genes coding for the plastid-encoded RNA polymerase. Planta 216(5):815–823.

Kristmundsson Á, Freeman MA. 2018. Harmless sea snail parasite causes mass mortalities in numerous commercial scallop populations in the northern hemisphere. Sci Rep. 8(1):7865.

Kristmundsson Á, Helgason S, Bambir SH, Eydal M, Freeman MA. 2011. Margolisiella islandica sp. nov. (Apicomplexa: Eimeridae) infecting Iceland scallop Chlamys islandica (Müller, 1776) in Icelandic waters. J Invertebr Pathol. 108(3):139–146.

Kwong WK, del Campo J, Mathur V, Vermeij MJA, Keeling PJ. 2019. A widespread coral-infecting apicomplexan with chlorophyll biosynthesis genes. Nature 568(7750):103–107.

Laetsch D, Blaxter ML. 2017. BlobTools: interrogation of genome assemblies. F1000Res 6:1287.

Lagesen K, et al. 2007. RNAmmer: consistent and rapid annotation of ribosomal RNA genes. Nucleic Acids Res. 35(9):3100–3108.

Langmead B, Trapnell C, Pop M, Salzberg SL. 2009. Ultrafast and memory-efficient alignment of short DNA sequences to the human genome. Genome Biol. 10(3):R25.

Lartillot N, Lepage T, Blanquart S. 2009. PhyloBayes 3: a Bayesian software package for phylogenetic reconstruction and molecular dating. Bioinformatics 25(17):2286–2288.

Leander BS, Ramey PA. 2006. Cellular identity of a novel small subunit rDNA sequence clade of Apicomplexans: description of the marine parasite *Rhytidocystis polygordiae* n. sp. (Host: *Polygordius* sp., Polychaeta). J Eukaryot Microbiol. 53(4):280–291.

Levine ND. 1979. Agamococcidiorida ord. n. and Rhytidocystidae fam. n. for the Coccidian genus *Rhytidocystis* Henneguy, 1907. J Protozool. 26(2):167–168.

Li D, Liu CM, Luo R, Sadakane K, Lam TW. 2015. MEGAHIT: an ultra-fast single-node solution for large and complex metagenomics assembly via succinct de Bruijn graph. Bioinformatics 31(10):1674–1676.

Li J, Maga JA, Cermakian N, Cedergren R, Feagin JE. 2001. Identification and characterization of a *Plasmodium falciparum* RNA polymerase gene with similarity to mitochondrial RNA polymerases. Mol Biochem Parasitol. 113(2):261–269.

Liere K, Weihe A, Börner T. 2011. The transcription machineries of plant mitochondria and chloroplasts: composition, function, and regulation. J Plant Physiol. 168(12):1345–1360.

Lim L, McFadden GI. 2010. The evolution, metabolism and functions of the apicoplast. Philos Trans R Soc B. 365(1541):749–763.

Mathur V, et al. 2019. Multiple independent origins of apicomplexan-like parasites. Curr Biol. 29(17):2936–2941.e5.

Mazumdar J, Striepen B. 2007. Make it or take it: fatty acid metabolism of apicomplexan parasites. Eukaryot Cell. 6(10):1727–1735.

McFadden GI, Reith ME, Munholland J, Lang-Unnasch N. 1996. Plastid in human parasites. Nature 381(6582):482–482.

Miroliubova TS, et al. 2020. Polyphyletic origin, intracellular invasion, and meiotic genes in the putatively asexual agamococcidians (*Apicomplexa incertae sedis*). Sci Rep. 10(1):10.1038/s41598-020-72287-x

Mungpakdee S, et al. 2014. Massive gene transfer and extensive RNA editing of a symbiotic dinoflagellate plastid genome. Genome Biol Evol. 6(6):1408–1422.

Muñoz-Gómez SA, et al. 2019. Nephromyces represents a diverse and novel lineage of the apicomplexa that has retained apicoplasts. Genome Biol Evol. 11(10):2727–2740.

Nguyen L-T, Schmidt HA, von Haeseler A, Minh BQ. 2015. IQ-TREE: a fast and effective stochastic algorithm for estimating maximum-likelihood phylogenies. Mol Biol Evol. 32(1):268–274.

Nisbet RER, McKenzie JL. 2016. Transcription of the apicoplast genome. Mol Biochem Parasitol. 210(1–2):5–9.

Patten R. 1935. The life history of *Merocystis Kathae* in the whelk, *Buccinum undatum*. Parasitology 27(3):399–430.

Picelli S, et al. 2014. Full-length RNA-seq from single cells using Smart-seq2. Nat Protoc. 9(1):171–181.

Price MN, Dehal PS, Arkin AP. 2010. FastTree 2 – approximately maximum-likelihood trees for large alignments. PLoS One 5(3):e9490.

Quang LS, Gascuel O, Lartillot N. 2008. Empirical profile mixture models for phylogenetic reconstruction. Bioinformatics 24(20):2317–2323.

Ralph SA, D'Ombrain MC, McFadden GI. 2001. The apicoplast as an antimalarial drug target. Drug Resist Updat. 4(3):145–151.

Rambaut A. 2014. FigTree v1.4.2, A Graphical Viewer of Phylogenetic Trees. Available from ⟨http//tree.bio.ed.ac.uk/software/figtree/⟩ [Internet] 1.4.2. Available from: http//tree.bio.ed.ac.uk/software/figtree

Roure B, Rodriguez-Ezpeleta N, Philippe H. 2007. SCaFoS: a tool for selection, concatenation and fusion of sequences for phylogenomics. BMC Evol Biol. 7(Suppl 1):S2.

Rueckert S, Leander BS. 2009. Phylogenetic position and description of *Rhytidocystis cyamus* sp. n. (Apicomplexa, Rhytidocystidae): a novel intestinal parasite of the north-eastern Pacific "stink worm" (Polychaeta, Opheliidae, Travisia pupa). Mar Biodiv. 39(4):227–234.

Sambrook J, Fritsch EF, Maniatis T. 1989. Molecular Cloning: A Laboratory Manual. 2nd ed. Cold Spring Harbor, NY: Cold Spring Harbor Laboratory Press.

Seeber F, Feagin JE, Parsons M. 2013. The Apicoplast and Mitochondrion of *Toxoplasma gondii*. In: Weiss L, Kim K, editors. *Toxoplasma Gondii*: The Model Apicomplexan - Perspectives and Methods. 2nd ed. Amsterdam: Elsevier. p. 297–350.

Sheiner L, Vaidya AB, McFadden GI. 2013. The metabolic roles of the endosymbiotic organelles of *Toxoplasma* and *Plasmodium* spp. Curr Opin Microbiol. 16(4):452–458.

Simão FA, Waterhouse RM, Ioannidis P, Kriventseva EV, Zdobnov EM. 2015. BUSCO: assessing genome assembly and annotation completeness with single-copy orthologs. Bioinformatics 31(19):3210–3212.

Slater GSC, Birney E. 2005. Automated generation of heuristics for biological sequence comparison. BMC Bioinformatics 6(1):31.

Smith DR. 2013. RNA-Seq data: a goldmine for organelle research. Brief Funct Genomics. 12(5):454–456.

Stamatakis A. 2014. RAxML version 8: a tool for phylogenetic analysis and post-analysis of large phylogenies. Bioinformatics 30(9):1312–1313.

Stoeck T, et al. 2010. Multiple marker parallel tag environmental DNA sequencing reveals a highly complex eukaryotic community in marine anoxic water. Mol Ecol. 19:21–31.

Su HJ, et al. 2019. Novel genetic code and record-setting AT-richness in the highly reduced plastid genome of the holoparasitic plant Balanophora. Proc Natl Acad Sci U S A. 116(3):934–943.

Teng CY, Dang Y, Danne JC, Waller RF, Green BR. 2013. Mitochondrial genes of dinoflagellates are transcribed by a nuclear-encoded single-subunit RNA polymerase. PLoS One 8(6):e65387.

Upton SJ, Peters EC. 1986. A new and unusual species of coccidium (Apicomplexa: Agamococcidiorida) from Caribbean scleractinian corals. J Invertebr Pathol. 47(2):184–193.

Votýpka J, Modrý D, Obornik M, Šlapeta J, Lukeš J. 2017. Apicomplexa. In: Archibald JM, Simpson AGB, Slamovits CH, editors. Handbook of the Protists. 2nd ed. Cham: Springer International Publishing. p. 567–624.

Watanabe N, et al. 2001. Dual targeting of spinach protoporphyrinogen oxidase II to mitochondria and chloroplasts by alternative use of two in-frame initiation codons. J Biol Chem. 276(23):20474–20481.

Wilson RJ, et al. 1996. Complete gene map of the plastid-like DNA of themalaria parasite *Plasmodium falciparum*. J Mol Biol. 261(2):155–172.

Zhang J, Kobert K, Flouri T, Stamatakis A. 2014. PEAR: a fast and accurate Illumina Paired-End reAd mergeR. Bioinformatics 30(5):614–620.

Associate editor: McFadden Geoff